Available online at www.sciencedirect.com

ScienceDirect

Procedia Structural Integrity 21 (2019) 215–223

Structural Integrity Procedia

www.elsevier.com/locate/procedia

1st International Workshop on Plasticity, Damage and Fracture of Engineering Materials

Investigation of fretting fatigue failure mechanism of lug-bush connection members

Emine Burcin Ozen[a], Yezdan Medet Korkmaz[a,b], Demirkan Coker[a,c]*

[a]*Department of Aerospace Engineering, Middle East Technical University, Ankara 06800, Turkey*
[b]*Turkish Aerospace Industries, Ankara 06800, Turkey*
[c]*METU Center for Wind Energy, Middle East Technical University, Ankara 06800, Turkey*

Abstract

Lug-bush connection members are widely used in aerospace industry, specifically in the connection of rotor to helicopter main body. Under small amplitude cyclic loadings, a fraction of the contact area experiences relative motion which causes fretting on the contacting surfaces. In this study, failure mechanisms of four different lug-bush members subjected to high cycle tensile fatigue loading are investigated. The contact surfaces are inspected using a digital microscope and a scanning electron microscope (SEM). Different surface regimes are observed at the mating surfaces which are shown to be the results of partial stick and slip of the contacting bodies. Energy dispersive spectroscopy (EDS) analysis in SEM showed that rubbing of lug-bush surfaces created wear debris at the sliding regions which then corroded and formed a tribolayer. A crack is observed to initiate in the vicinity of tribolayer boundary. FEA of these members are carried out using ABAQUS by defining interference and contact to mating surfaces of the lug and bush. The results showed qualitative agreement with the experimental investigations in terms of peak slip locations.

Peer-review under responsibility of the 1st International Workshop on Plasticity, Damage and Fracture of Engineering Materials organizers

Keywords: fretting fatigue; tribolayer; sticking-sliding regions

* Corresponding author. Tel.: +90-312-210-4257; fax: +90-312-210-4250.
E-mail address: coker@metu.edu.tr

Peer-review under responsibility of the 1st International Workshop on Plasticity, Damage and Fracture of Engineering Materials organizers
10.1016/j.prostr.2019.12.104

1. Introduction

Fretting fatigue is a surface phenomenon which occurs in the mating surfaces of two contacting bodies under small amplitude vibrations. The necessary condition for fretting to occur is $Q(t) < \mu P$, where $Q(t)$ is the applied cyclic tangential force, P is the applied constant normal force, and μ is the friction coefficient of the corresponding contact surfaces, as shown in Fig. 1 (Goryacheva et al. (2001), Vingsbo (1992)). Since the applied tangential load is not able to overcome the force required to create a bulk motion, only a fraction of the contact area experiences relative motion. Therefore, sticking and sliding regions are formed depending on the existence of relative motion between mating surfaces.

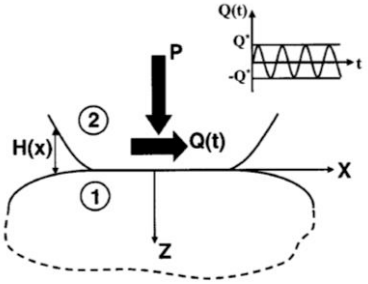

Fig. 1. Schematic view of the contact area of two elastic bodies subjected to a normal force P and an oscillatory tangential force Q(t) (Goryacheva et al. (2001)).

Fretting fatigue failure is observed in lug-bush connection members, which are used widely in the aerospace industry. An example of the usage area of lug-bush connection members is the rotor and body connection of helicopters, as shown in Fig. 2. These connection members are assembled together using interference fit method. Fretting fatigue is also observed in dovetails of jet engine parts and artificial hip joints (Szolwinski and Farris (1996)).

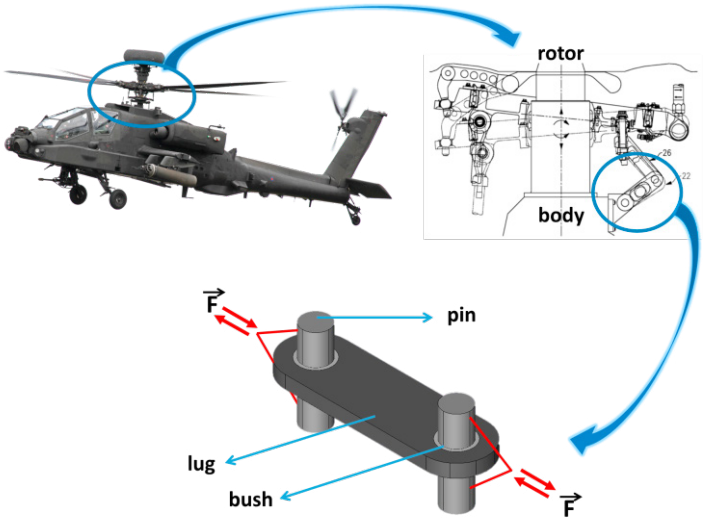

Fig. 2. Usage of lug-bush connection members in helicopters.

The objective of this study is to investigate the failure mechanism of different lug-bush connection members. This study focuses on tribolayer formation, fracture location, and sticking-sliding surface characteristics. Investigated lug-bush members are made of Ti and Al lugs with Al and steel bushes and subjected to high-cycle tensile fatigue loading. Three steel bushes were combined with two Ti lugs (specimens A and B) and one Al lug (specimen C), and in addition, an Al bush was combined with an Al lug (specimen D), as shown in Fig. 3, using interference fit.

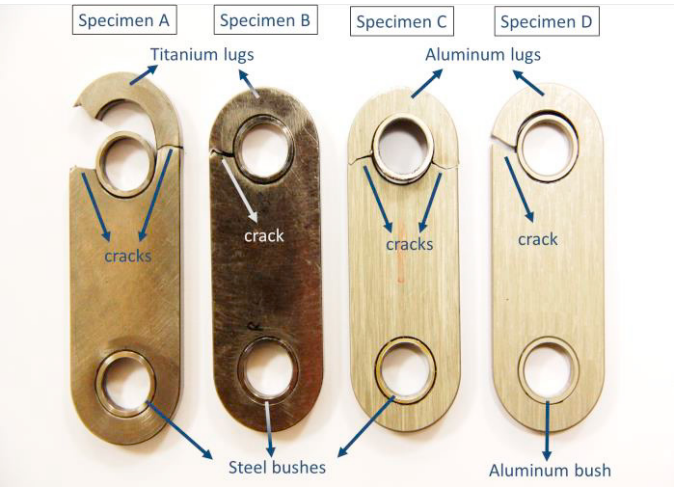

Fig. 3. Investigated lug-bush connection members, made of Ti and Al lugs with Al and steel bushes.

2. Method

Photographs of the failed lug-bush connection members are taken using a camera with macro lenses. Black residues lying discontinuously in the direction of the cyclic loading are observed on the surfaces of both lug and bush. Matching surfaces of the lug and bush are detected with the help of these pictures and residues. Fig. 3 shows the crack locations of the lugs. Using the matching residues on the lug and bush surfaces, the corresponding location of the cracks are identified on bush surfaces.

A digital microscope, Huvitz HDS 5800, is used to investigate the surfaces at high magnifications. In addition, extending depth of field (EDF) feature of the digital microscope is used. This feature enables the observer to see the 3-D surface shapes and qualities.

Scanning electron microscope (SEM) is used for further observations of the surface as well as the determination of the elemental composition, using energy dispersive spectroscopy (EDS) analysis. Energy dispersive spectroscopy analysis is a method to detect the elemental composition of the analyzed surface using electron beams.

3. Results and Discussion

3.1. Investigation of Ti Lug – Steel Bush Members

Under tensile fatigue loading of investigated lug-bush connection members, failure occurred at high number of cyclic tensile loads. The observed lug-bush members are made of Ti lugs with steel bushes (specimens A and B) as shown in Fig. 3. A crack initiated at the contacting surface of the lug and bush, leading to fracture of the lug. Investigations of the contact surfaces revealed black residues both on the lug and bush surfaces, as shown in Fig. 4-a.

Observations of the lug and bush mating surfaces using both camera and digital microscope revealed that the fracture of the lug of specimen A occurred near the boundary of an intense residue and a clean surface, as shown in Fig. 4-b. The two distinct regions of black residues and clean parts raised the question of whether the residues are product of relative motion and the clean parts are product of sticking of the contacting surfaces.

To answer that question, surface of the steel bush is investigated under digital microscope using extending depth of field (EDF) feature. The EDF analysis of the residues exhibited a rough surface whereas the clean parts were quite smooth. These analyses indicated that the relative motion of the contacting surfaces of the lug and bush created a wear debris which is observed as a rough surface under digital microscope. On the other hand, the clean parts had no evidence of a relative motion. These surfaces stuck together during the cyclic tensile loading, resulting in a clean surface and smooth appearance. As a result, the region with residues and the clean region are called sliding and sticking

regions, respectively. Also note that the sticking and sliding regions in Fig. 4 are not composed of two different photographs, the boundary of these regions is very sharp.

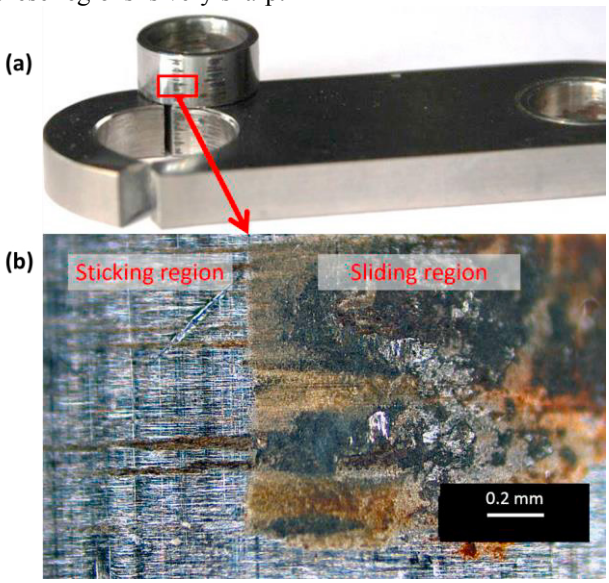

Fig. 4. (a) The photograph of the matching lug-bush surfaces, (b) Boundary of the sticking and the sliding regions on the steel bush surface under digital microscope at 200x magnification.

After discussing the reasons for different surface regimes, the color of these two distinct regions were the second question to be answered. Although the color of the residues looked like a corroded surface under the digital microscope at 500x magnification as shown in Fig. 5, scanning electron microscope (SEM) is used to further investigate the differences in sticking and sliding regions on the surface of the bush.

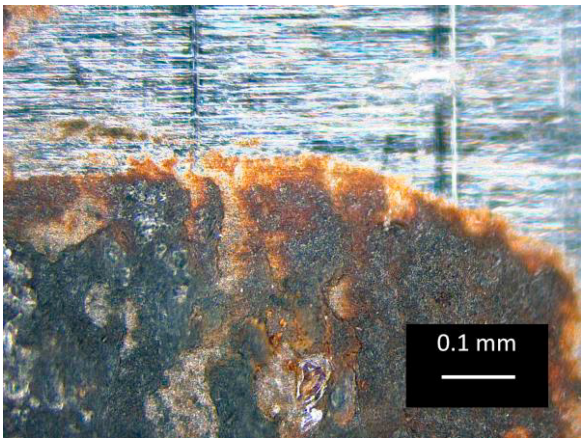

Fig. 5. Sliding region (at the bottom) on the steel bush surface, showing black residues, under digital microscope at 500x magnification.

SEM image of the residues on the steel bush surface is shown in Fig. 6. The surface which represents the sliding region is not smooth and the wear can be observed. Furthermore, one can realize that the SEM photograph of the worn surface, in Fig. 6, is very similar to a typical corroded surface appearance. In order to determine the differences between sticking and sliding regions in terms of elemental composition, EDS analysis is conducted. According to the results of the EDS analysis, sliding regions contain high amount of oxygen whereas the sticking regions do not have any oxygen content.

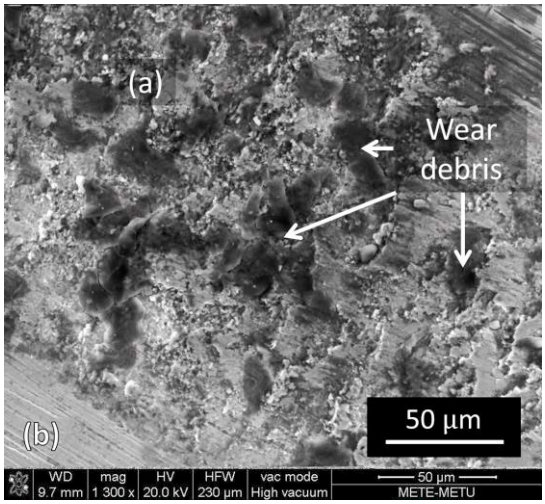

Fig. 6. SEM photograph showing (a) sliding region and (b) sticking region on the steel bush surface at 1300x magnification.

Macro and micro observations are certified with these results concluding that the worn surfaces oxidized and attained a black-brown color, which are referred as black residues in the observations. EDS results show that 20 % (by mass) oxygen exists within the residues as shown in Fig. 7-a. On the other hand, the clean surfaces in other words sticking regions did not experience relative motion of the contacting surfaces. In these regions, the black-brown residues were not observed. EDS results revealed that no oxygen content was detected in the sticking regions as shown in Fig. 7-b.

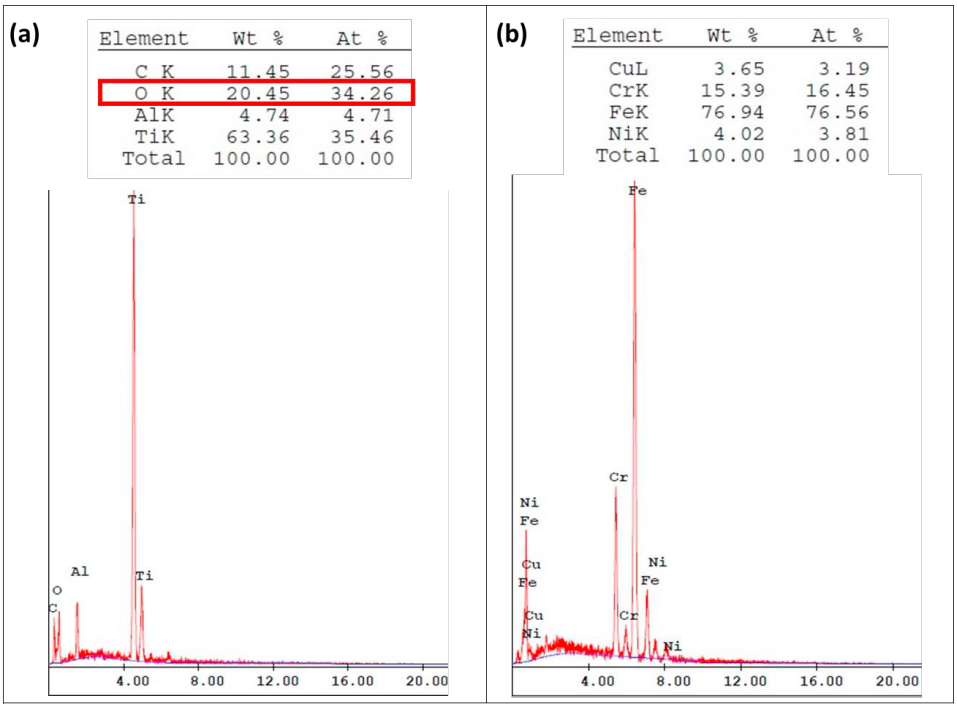

Fig. 7. EDS analysis results of (a) sliding region and (b) sticking region on the steel bush surface.

These results indicate that the oxidation of wear debris occurred at the sliding region, which is called tribolayer, as stated in Blau (2009). The tribolayer contains fine metallic particles from the two contacting surfaces as well as oxides. The frictional behavior of the two contacting surfaces are determined by the characteristics of the formed tribolayer, as discussed in Iwabuchi (1991).

3.2. Investigation of Sticking and Sliding Regions of Lug – Bush Members

Sticking-sliding regions of the four different lug-bush members are compared. The shape of tribolayer appearances of specimens A, B, and C, which have dissimilar lug and bush materials, are observed to be directional and discontinuous as shown in Fig. 8-a. However, in Al lug – Al bush member (specimen D) the surface features of the bush include rounded residues, as shown in Fig. 8-b.

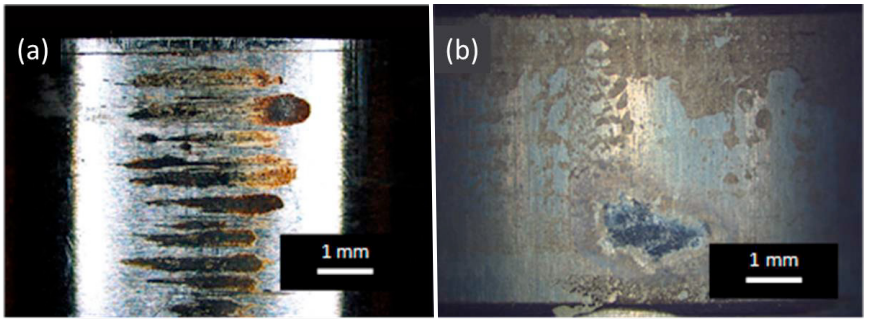

Fig. 8. The sliding region morphologies on the bush surfaces of (a) Ti lug – steel bush member (specimen A) and (b) Al lug – Al bush member (specimen D), at 50x magnification.

Locations of fracture and sticking-sliding regions of these four members made of Ti and Al lugs with Al and steel bushes are mapped as shown in Fig. 9. The red lines in the maps represent the sliding regions where black residues of the oxidized wear debris is observed on the contacting lug and bush surfaces. Remaining surfaces were free from any residues and are represented with blue, indicating the sticking surfaces.

A crack was found to initiate near the boundary of sticking and sliding regions after which it propagated, breaking one side of the lug. The boundary location of the sticking and sliding regions lies at 100° - 105°, as shown in Fig. 9. The reason for the difference in sliding region representation in Fig. 9-c is the rounded tribolayer shape.

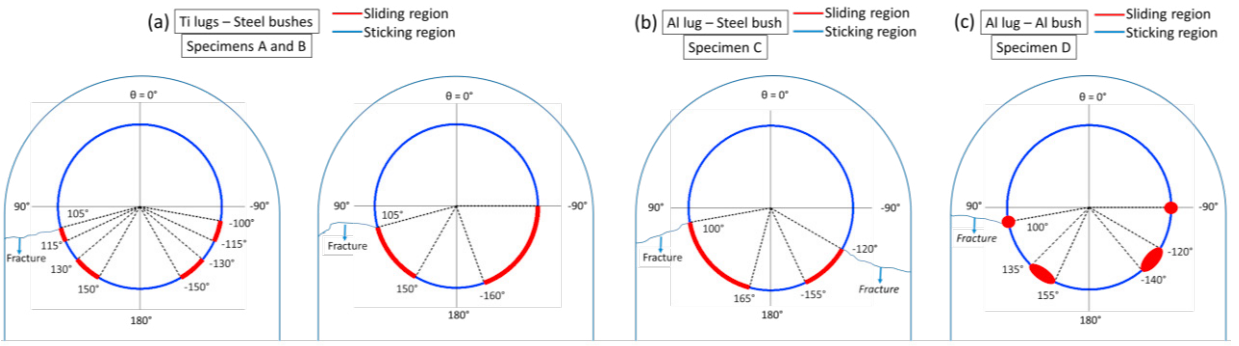

Fig. 9. Location of fracture and sticking-sliding surfaces of tested (a) Ti lug – steel bush members, (b) Al lug – steel bush member, and (c) Al lug – Al bush member.

3.3. Finite Element Analysis (FEA) of the Lug-Bush Members

3-D finite element model of statically loaded lug-bush assembly is generated using ABAQUS/Standard. Half of the lug and bush are modelled separately using their original dimensions, where the outer bush diameter is greater than the inner lug diameter. Both parts are discretized with 8-noded 3-D linear solid elements (C3D8 from ABAQUS library), as shown in Fig. 10-a. The symmetry surface of the lug is fixed in the loading direction, as shown in Fig. 10-b. The analysis is performed in two steps. In the first step, the interference of the bush into the lug is defined by enabling automatic shrink fit option of the ABAQUS/Standard with gradual remove of the slave node overclosures. Prior to second step, a contact between the inner walls of the lug hole and outer surface of the bush is defined by using master-slave algorithm with a prescribed friction coefficient of 1. During the second step, a pressure distribution with a magnitude of 4000 MPa in cosine form is applied to the upper inner surface of the bush. The magnitudes of the friction coefficient and pressure distribution are chosen by trial and error such that the sticking and sliding regions agree with the experimental results qualitatively.

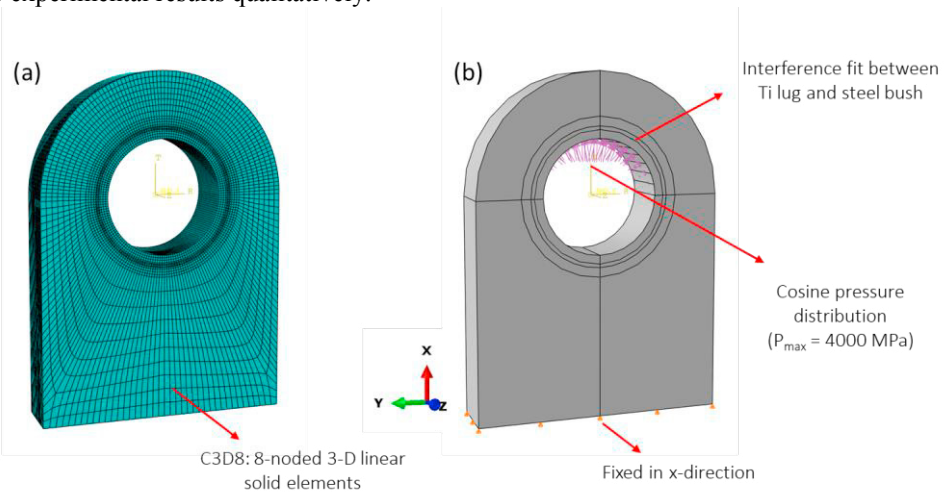

Fig. 10. FE model showing (a) meshing and (b) loading and boundary conditions of the lug and bush member.

Fig. 11 shows the von Misses stress contours in the Ti lug at the end of the first and second steps. The compressive residual stresses at the lug opening after the interference of the bush is shown in Fig. 11-a. The stress level at the bottom half of the lug increases, as shown in Fig. 11-b, after the load is applied.

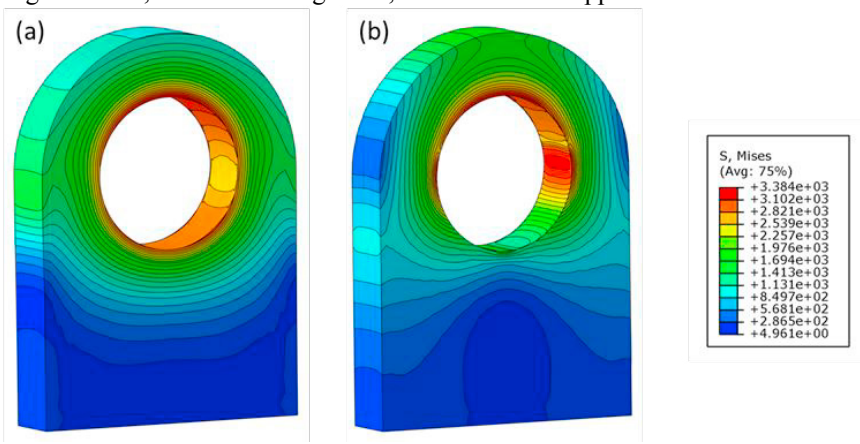

Fig. 11. Von Misses stress contours in the Ti lug at the end of (a) first step and (b) second step of the analysis.

Relative slip amplitude between the contacting surfaces of Ti lug and steel bush at the end of second step is shown in Fig. 12-a. The slip amplitude is provided as an output when contact is defined through master-slave algorithm and it is defined as the relative nodal displacement between the nodes of the mating surfaces (ABAQUS Analysis User's Manual (2011)). The slip amplitude is plotted against the position around the contacting Ti lug – steel bush surface, as shown in Fig. 12-b. Slip amplitude is symmetric with respect to $\theta = 0°$ and it reaches its maximum value around 115° and 245° (or in -115°).

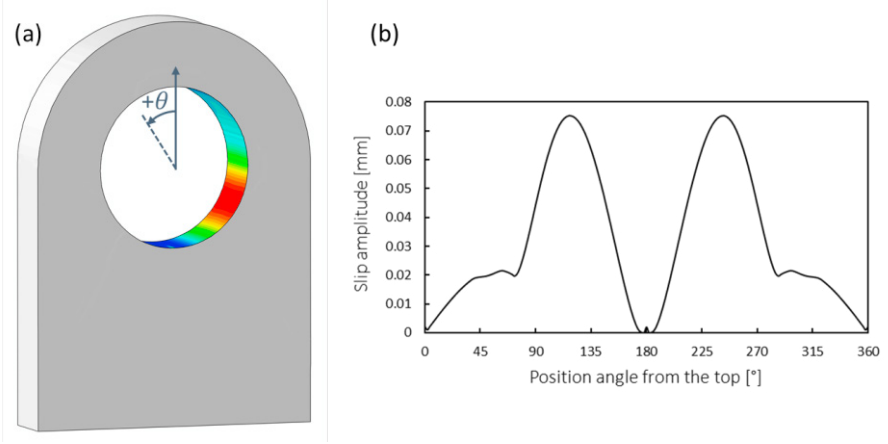

Fig. 12. Slip amplitude around the contacting Ti lug – steel bush surface (a) shown on the lug model and (b) with respect to position angle from the top.

These results agree with the aforementioned observations of the fractured lug – bush members, since the residues are observed around the peak slip amplitude locations.

4. Conclusions

Under tensile fatigue loading certain parts of the contacting surface of the lug and bush interface experience relative sliding while some parts of the contacting surface remain still with respect to each other. In sliding regions, the surfaces rub against each other and create a wear debris. As the oxidation of the wear debris takes place, a resulting product composed of fine metal particles and oxides is formed. This residual product is called a tribolayer. In sticking regions no wear debris forms therefore the surface remains clean and smooth. The sticking regions can be differentiated from the sliding regions easily with both macro and micro investigations due to black-brown color of the tribolayer.

Four different lug-bush members are investigated and a specific location has been detected for the crack initiation. As observed at all specimens, fracture starts at the vicinity of the sticking and sliding region boundary, approximately at 100°.

FEA results show good qualitative agreement with the experimental investigations. The peak slip amplitude regions lie approximately at ±115°. The tested lug – bush members include this peak amplitude location in the sliding regions.

Different parameters affecting the result of finite element analysis such as the applied load, friction coefficient, interference pressure etc. are topics for the future work.

Acknowledgements

We would like to thank Baran Guler and Assist. Prof. Dr. Mert Efe at the Department of Metallurgical and Materials Engineering who helped us with the SEM and EDS analyses.

References

Blau, P. J., 2009. Friction Science and Technology, from Concepts to Applications. CRC Press/Taylor & Francis Group, Boca Raton, pp. 188.

Goryacheva, I. G., Rajeev, P. T., Farris, T. N., 2001. Wear in partial slip contact. Journal of Tribology, 123, 848-856.
Iwabuchi, A., 1991. The role of oxide particles in the fretting wear of mild steel. Wear 151, 301–311.
Nishioka, K., Hirakawa, K., 1969. Fundamental Investigations of Fretting Fatigue (Part 3, Some Phenomena and Mechanisms of Surface Cracks). Bulletin of JSME 12, 397-407.
Simulia. ABAQUS 6.11 - Analysis User Manual. Providence (RI, USA); 2011.
Szolwinski, M. P., Farris, T. N., 1996. Mechanics of fretting fatigue crack formation. Wear 198, 93-107.
Varenberg, M., Halperin, G., Etsion, I., 2002. Different Aspects of the Role of Wear Debris in Fretting Wear. Wear 252, 902-910.
Vingsbo, O., 1992. Fretting and Contact Fatigue Studied with the Aid of Fretting Maps, in Standardization of Fretting Fatigue Test Methods and Equipment, edited by Attia, M., Waterhouse, R.. ASTM International, 49-59.